Vailable online at www.sciencedirect.com

SciVerse ScienceDirect

Energy Procedia 27 (2012) 53 – 58

Energy Procedia

SiliconPV: April 03-05, 2012, Leuven, Belgium

Influence of Base Resistivity on Solar Cell Parameters of Double-side Contacted Rear Junction Solar Cells

V. Mertens[a*], T. Ballmann[a], J. Y. Lee[a], M. Junghänel[a], F. Stenzel[a], L. Brandt[a,b], A. Schulze[a], P. Engelhart[a], J. W. Müller[a], P. Wawer[a], and K. H. Küsters[a]

[a]*Q-Cells SE, Sonnenallee 17-21, D-06766 Bitterfeld-Wolfen, Germany*
[b]*Martin-Luther-University Halle-Wittenberg, Institute of Physics, Photovoltaics Group, Van-Danckelmann-Platz 3, 06120 Halle/Saale, Germany*

Abstract

We study the dependence of solar cell parameters on base resistivity for double-side contacted *n*-type rear junction solar cells with boron emitter and local rear contacts. Experimental data for solar cells processed on *n*-type Cz Si wafers with base resistivities ranging from 2 Ω·cm to 16 Ω·cm are compared to device simulations for the respective resistivity range. Our experimental data show the typical strong increase of efficiency with base resistivity in the range of 2 - 5 Ω·cm and at about 10 Ω·cm a saturation of efficiency with base resistivity sets in [1, 2, 3, 4].
Comparison of experimental and simulation results reveal that our experimental findings are closely reproduced assuming a constant bulk lifetime after solar cell processing. Furthermore the results of this study were implemented in an optimized solar cell process. With 14 Ω·cm *n*-type Cz as base material solar cell efficiencies of up to 20.9% on 243.4 cm² (total area) were achieved which was confirmed by Fraunhofer ISE CalLab.

Keywords: *n*-type silicon; base resistivit; rear junction solar cell

1. Introduction

In order to improve efficiencies of double-side contacted solar cells on Czochralski (Cz) silicon base material, recently the interest in respective solar cell concepts which use *n*-type Cz silicon has increased [5]. *N*-type Cz silicon exhibits high minority carrier lifetimes and is more tolerant towards various metal impurities than *p*-type Cz [6, 5]. Due to the high bulk lifetime of the *n*-type Cz material, the *p*-*n* junction can be placed either on the front or rear side of the solar cell. Our approach is a rear junction solar cell structure using a diffused boron emitter [6, 7]. Double-side contacted solar cells with a rear junction and

* Corresponding author. Tel.: +49 (3494) 6699 - 52120; fax: +49 (3494) 6699 - 51012.
E-mail address: v.mertens@q-cells.com.

doi:10.1016/j.egypro.2012.07.028

an aluminum p^+-emitter have been reported earlier [1, 2, 4, 6, 9, 10]. Both rear junction variants exhibit a phosphorus diffusion on the front side. Therefore all innovations developed for front side metallization of *p*-type solar cells can be applied to a rear junction cell structure on *n*-type silicon, as well.

Commonly, base material with high resistivity is used as this leads to maximum solar cell efficiencies. In this article we investigate the influence of resistivity for double-side contacted rear junction solar cells with boron emitter on experimental basis to quantify the efficiency losses caused by non-optimum base resistivity. We also compare our data to 1D solar cell device simulations in order to test two different assumptions concerning the bulk lifetime versus resistivity dependence after solar cell processing for our experimental solar cells.

2. Experimental

The double-side contacted *n*-type Si rear junction silicon solar cells investigated within this article are prepared by typical high efficiency processing methods using thermal silicon dioxide as diffusion barrier for single side phosphorus and boron tube furnace diffusions. The front and the rear side of our solar cells are passivated by dielectric layers. The front side metallisation is realised by screen printing and light induced Ag-plating. For the rear side metallisation point contact openings and aluminium deposited by physical vapour deposition are used. The distance of front grid fingers is held constant for all resistivities. As base material we processed wafers from two different *n*-type Czochralski silicon ingots with base resistivity ranges from 2 to 6 Ω·cm and 6 to 16 Ω·cm. The wafer size is 15.6·15.6 cm^2 (full square) and the wafer thickness is 200 µm. A cross section of our rear junction solar cell is shown in Fig 1a.

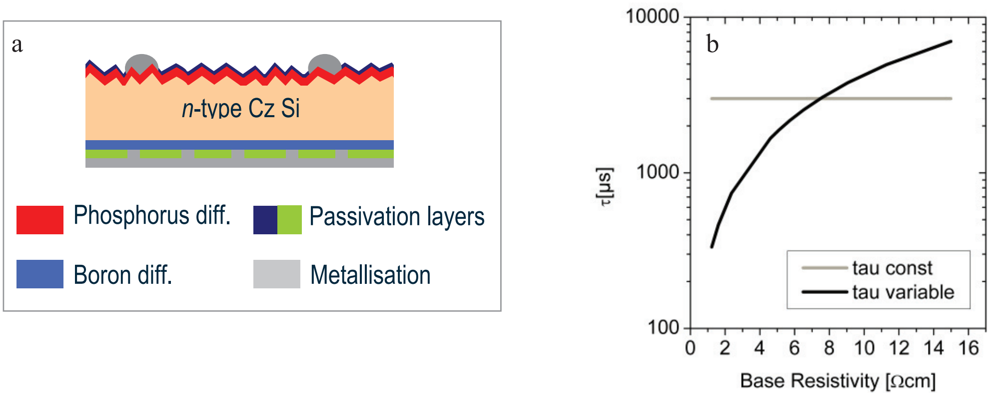

Fig. 1. a: Cross section of the double-side contacted rear junction solar cell investigated within this article; 1b: diagram of the two bulk lifetime on base resistivity assumptions after solar cell processing taken for the 1D device simulations: case 1: constant lifetime of 3 ms; case 2: bulk lifetime increases with increasing resistivity

In order to compare our experimental findings to device simulations we used the numerical device simulation tool PC1D [11]. Simulations were performed for the range of base resistivities of our experimental data. For the diffused front and rear, parameterizations of experimental diffusion profiles are used. The front reflection is considered using experimental data, too. Surface recombination velocities, diode non-idealities and resistance effects are adjusted to give similar results as experimental solar cells. The simulations tested for two hypothetical minority carrier bulk lifetime (final device) vs. resistivity dependencies: As first case, the bulk lifetime is considered to be limited by the solar cell process and thus independent of base resistivity. Here we assume a constant lifetime of 3 ms after processing. As second case, we take the bulk lifetime to increase with base resistivity. As reference data for our lifetime on resistivity dependence, minority carrier lifetime results prior to high temperature processing are used from in-house measurements. Figure 1b shows the two lifetime cases considered in the simulations. After the simulations and their interpretation the most appropriate resistivity determined by our study was chosen for an optimized solar cell process and a new set of solar cells was produced.

3. Results and Discussion

The variation of solar cell parameters with base resistivity of our experimental solar cells is shown in Figure 2a-d as open and closed circles. Simulation results for the two assumed lifetime-resistivity dependencies are shown in the same graphs as lines.

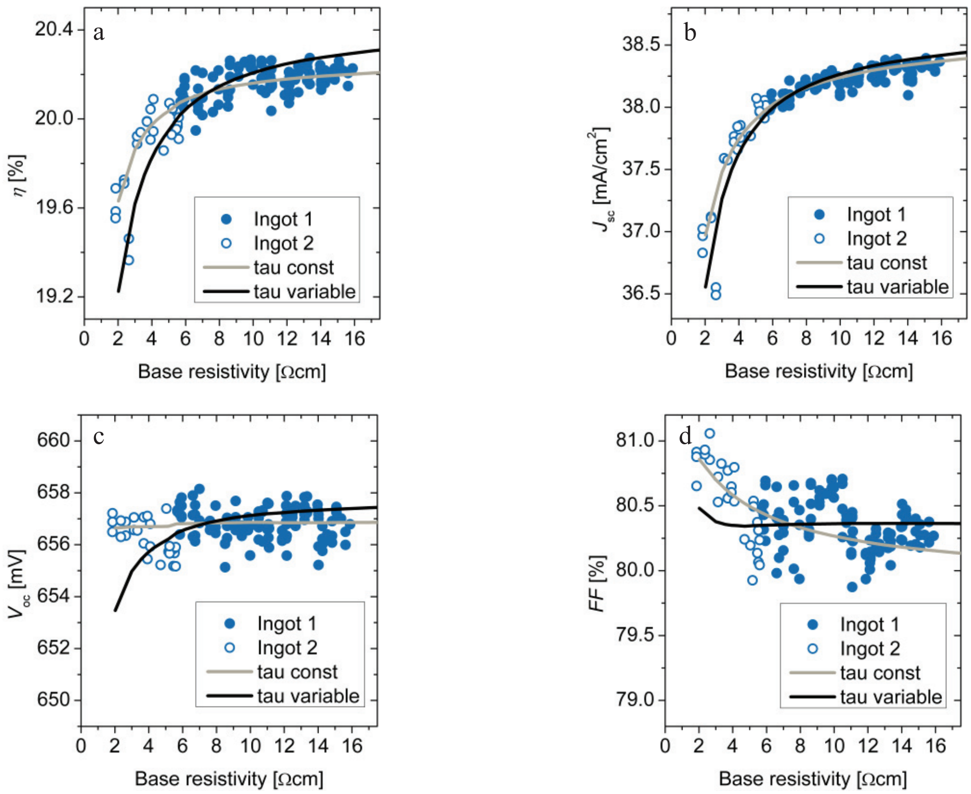

Fig. 2. Experimental data and simulations: dependence of solar cell parameters (a: efficiency η , b: short circuit current density J_{sc}, c: open circuit voltage V_{oc}, and d: fill factor *FF*) for double-side contacted rear junction solar cells on base resistivity. For the simulations two different cases for the bulk lifetime dependence on resistivity are considered: case 1: constant lifetime of 3 ms; case 2: increasing lifetime with increasing resistivity

For the experimental results a strong dependence of solar cell efficiency on base resistivity from 2 Ω·cm to 5 Ω·cm is observed (Fig 2a). From about 5 Ω·cm the dependence of efficiency on base resistivity is significantly reduced and at about 10 Ω·cm a saturation sets in. This efficiency dependence on base resistivity is mainly caused by the short circuit current density (J_{sc}): the data in Fig 2b reveal a strong increase in J_{sc} with increasing base resistivity in the range of 2 Ω·cm to 5 Ω·cm. The J_{sc} is also responsible for the reduced efficiency dependence on resistivity above 5 Ω·cm (Fig 2b). The experimental open circuit voltage data (V_{oc}) show no significant change with base resistivity (Fig 2c). The fill factor data (*FF*) show a relatively small decrease with increasing resistivity of about 1% abs (Fig 2d).

The comparison of our experimental and simulation data are also shown in Figure 2a-d. To adjust the simulation results to our experimental findings we used an S_{front} value of 6000 cm/s and an S_{rear} value of 1800 cm/s. The experimental solar cell parameters for different base resistivities resemble closely the simulated dependence on base resistivity determined for a constant bulk lifetime after processing. This is clearly seen from the simulated dependence of the V_{oc} and the *FF* on base resistivity: the simulated case 1 (constant bulk lifetime) exhibits a constant V_{oc} and a decreasing *FF* with increasing resistivity, which is in accordance with our experimental findings. However the simulated case 2 (increasing bulk lifetime with increasing resistivity) results in increasing V_{oc} and from 4 Ω·cm on a constant *FF* with increasing resistivity is observed which is not seen experimentally. The dependence of J_{sc} on resistivity gives the same trend of increasing J_{sc} with increasing resistivity for both cases but the dependence is somewhat more pronounced for case 2. It should be emphasized that our findings might be specific for our solar cell process and the Cz material used. Other silicon materials for instance *n*-type float zone material might not show this constant, "process limited" lifetime behaviour.

We also verified our 1D simulation data with Synopsis Sentaurus 3D simulations and obtained the same dependencies for J_{sc} and V_{oc} as from PC1D [12]. Concerning the fill factor the different behaviour of the case 1 (constant lifetime) and case 2 (varying lifetime) is even more pronounced in 3D simulations than in 1D: for the constant lifetime (case 1) the fill factor decreases with increasing resistivity in accordance with 1D simulations, for the varying lifetime (case 2) the *FF* even increases with resistivity (data not shown).

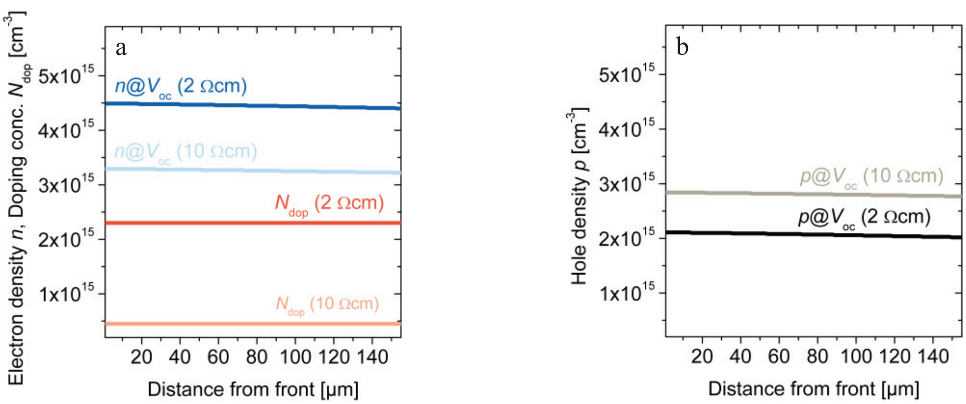

Fig. 3. PC1D simulation of carrier densities within the bulk for 2 and 10 Ω·cm base material at V_{oc} conditions (case 1: constant bulk lifetime of 3 ms). a: Comparison of electron densities *n* and doping concentrations N_{dop}, b: hole densities *p*

Comparing our experimental results to earlier investigations in literature we find that the saturation of efficiency for resistivities of 10 Ω·cm or higher is in accordance with simulations for Al p^+-emitter rear junction solar cells [1, 2, 4]. In order to explain the strong dependence of J_{sc} on resistivity on the one hand and the constant V_{oc} on the other hand, we first take a closer look on the n^+-n high-low junction at the front side of our solar cell. The higher the difference in doping densities of n^+-diffusion and *n*-base region the more effective is the shielding effect of the n^+-diffusion on the minority carriers at the front side that means consequently a reduction of the front side recombination. Therefore the J_{sc} increases with increasing bulk resistivity. This influence of base resistivity on the passivation quality of n^+-n high low junctions was shown by device simulations for lowly doped front surface field [3, 4] but was also experimentally observed for 45 Ω/sq and 65 Ω/sq phosphorus diffusions [1, 4]. The open circuit voltage however does not change with resistivity. This can be understood considering that at V_{oc} conditions the bulk is in high-level injection (HLI). Even 2 Ω·cm base material is in transition to HLI at V_{oc} conditions. This situation is illustrated in Fig. 3a and b: for 2 Ω·cm base material, the electron density n (dark blue line in Fig. 3a) is already by a factor of 2 higher than the doping concentration (red line in Fig. 3a) indicating the transition to HLI. For 10 Ω·cm base material the electron density (light blue line in Fig 3a) is even one order of magnitude larger than the doping concentration (yellow line in Fig. 3a). The hole densities p at V_{oc} conditions for the 2 Ω·cm and 10 Ω·cm base material are given in Fig. 3b. Assuming a constant bulk lifetime for all resistivities and considering the discussed HLI conditions lead to open circuit voltages which are independent of the resistivity. However if the bulk lifetime is assumed to increase with resistivity, an open circuit voltages dependence on resistivity is reintroduced again. The aforementioned considerations about HLI conditions are still valid but the V_{oc}-dependence is now dominated by the effect of variation in bulk lifetime.

In order to evaluate the potential of this solar cell structure we processed a new set of solar cells on high ohmic n-type Cz material (14 Ω·cm) including additional improvements on the front passivation and front metallisation which were determined from other investigations not shown here. Our best solar cell achieved an efficiency of 20.9% on 6 inch full square wafer format which results in an output power of 5.09 W. This result was independently confirmed by ISE CalLab. Figure 4 shows the *I-V* characteristic of this solar cell and the respective cell parameters.

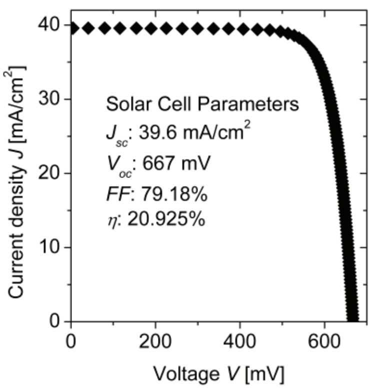

Fig. 4. *I-V* characteristic and solar cell parameters of our best solar cell with efficiency of 20.9% and 5.09 W output power processed with optimized base resistivity of 14 Ω·cm (Confirmation by Fraunhofer ISE CalLabConclusions

4. Conclusion

In this article we present experimental solar cell data for the variation of base resistivity of double-side contacted rear junction solar cells. Our data reveal the resistivity distribution is mainly influenced by the behavior of short circuit current density. In the range of 2 to 5 Ω·cm a strong increase in short circuit current density and therewith also in efficiency is detected due to improvement of passivation quality of the front side high-low n+-n junction with increasing bulk resistivity [3]. From 5 Ω·cm base resistivity on only small variation in short circuit current density and efficiency is present. Ingots with resistivity distributions from 5 to 16 Ω·cm can therefore be processed to double-side contacted rear junction solar cells with only minor variation in efficiency.

Comparison of the experimental ingot distributions to respective simulation data shows the bulk lifetime after solar cell processing is appropriately approximated assuming a constant bulk lifetime for all resistivities. With a base resistivity of 14 Ω·cm we processed a new set of solar cells with improved front passivation und metallization. The best cell had an efficiency of 20.9% which was confirmed by Fraunhofer ISE CalLab.

Acknowledgements

This work is supported by the German Ministry for Environment, Nature Conservation and Nuclear Safety (BMU) under Contract No. 0329988C ("ALBA II").

References

[1] T. Buck, J. Libal, S. Eisert, R. Kopecek, K.O. Peter, K. Wambach, *Proceedings of 19th European Photovoltaic Solar Energy Conference* , Paris, 2004.

[2] R. Kopecek et al., *Proceedings of the 4th IEEE World Conference on Photovoltaic Energy Conversion*, Waikoloa, Hawaii, 2006.

[3] M. Hermle, F. Granek, O. Schultz, S.W. Glunz, *Journal of Applied Physics*, 2008, **103**, 054507.

[4] H. Nagel et al., *Proceedings of the 21th EUPVSEC*, Dresden, Germany, 2006.

[5] 1st nPV workshop, Constance, Germany, 2011.

[6] J. Schmidt, K. Bothe, R. Bock, C. Schmiga, R. Krain, R. Brendel, *Proceedings of the 22nd EUPVSEC*, Milan, Italy, 2007.

[7] X.M. Dai, M.A. Green, S.R. Wenham, *Proceedings of the 23rd IEEE PVSC*, Louisville, Kentucky, 1993.

[8] S. Bordihn et al., *Proceedings of the 26th EUPVSEC*, Hamburg, Germany, 2011.

[9] C. Schmiga, H. Nagel, J. Schmidt, Progress in Photovoltaics, 14, 533-539, 2006.

[10] C. Schmiga et al. *Proceedings of the 25th EUPVSEC*, Valencia, Spain, 2010.

[11] P.A. Basore, D.T. Rover, and A.W. Smith, *Proceedings of the 20th IEEE PVSC*, 1988.

[12] SENTAURUS, Version D-2010.03, Synopsys Inc. Mountain View, CA (www.synopsys.com/products/TCAD/TCAD.html).